

Spatial rotational temperature and emission intensity profiles in silane plasmas

Spyros Stamou, Dimitris Mataras and Dimitris Rapakoulias

Laboratory of Plasma Chemistry, Department of Chemical Engineering,
University of Patras, PO Box 1407, 26500, Patras, Greece

Received 5 February 1998, in final form 28 July 1998

Abstract. The spatial variation of the rotational temperature of the 0–0 band of the $A^2\Delta \rightarrow X^2\Pi$ transition of SiH in radio frequency pure silane discharges is investigated by utilizing a method of improved accuracy for the simulation of the emission spectrum. Furthermore, the variation of the rotational temperature as a function of the pressure at the maximum intensity position of the interelectrode space is examined. The results are used to extract information about the relative variations of the electron energy distribution function and the effective electron density in the interelectrode space. Thus, it is considered that there is a sensitive relation of the observed high rotational temperatures to the mean electron energy, provided that the electron energy distribution function does not change. More specifically, a decrease of the rotational temperature is observed on moving away from the powered electrode sheath region and a similar decrease is also detected with increasing pressure. This behaviour is compared with the spatial emission intensity profiles. The variation of the space-integrated emission intensity under the various discharge conditions, related to the modification of the effective electron density, is also presented.

1. Introduction

The applicability of low-pressure gas discharges for the deposition or treatment of materials has attracted the attention of researchers to some of the fundamental aspects of these processes [1, 2]. One of these cases concerns silane discharges which are widely used, especially in the microelectronics industry, for the deposition of various types of thin films [3]. Despite the effort and the application of various plasma diagnostic techniques, up to now, there is a lack of information concerning the number density and the energy of the various species involved therein. The situation is even more complicated if one takes into account that all the microscopic plasma parameters are also sensitive functions of space and time. Most of the past studies have applied optical diagnostics for obtaining the absolute densities of species or relative concentrations as a function of space and/or time [4–7]. The determination of the energy content of these species has not been researched equally, after some early works, due to its difficulty [8]. The interesting aspect is that all the studies performed in silane discharges up to now indicate that there is a high rotational–vibrational excitation of the molecular fragments resulting from the electron impact dissociation or dissociative excitation of silane. Perrin and Delafosse [8] have reported a rotational temperature ranging from around 1500 to 2000 K and

a vibrational temperature of around 4000 K. Similar results have been obtained by Tsurubuchi *et al* [9], who additionally observed an increase of vibrational excitation and a decrease of rotational excitation with increasing electron impact energy. In addition, the study of the translational energy distribution of excited hydrogen atoms, which are also created through electron impact dissociation of silane, has shown that there is a systematic dependence of the kinetic energy of the resulting fragment on the electron impact energy [10]. Thus, it is considered that more than 90% of the excess energy is imparted to ‘hot’ hydrogen atoms as translational energy [11]. In keeping with this trend, it is reasonable to assume that the mean electron energy has an influence on the rotational temperature of $\text{SiH}^*(A^2\Delta)$ exhibited in silane glow discharges. If this is true, then the pressure dependence of the electron energy distribution function (EEDF) would induce a similar behaviour to the rotational temperature. On the basis of these observations, a simple analogy between the mean electron energy and the rotational temperature appears a sensible approach as a first step to develop a non-perturbing space–energy sensitive technique for plasma diagnostics. However, to the best of our knowledge there are no data in the literature published up to now concerning the dependence of the rotational temperature on the discharge conditions or its spatiotemporal dependence.

Various techniques have been used to measure rotational and vibrational temperatures of excited or ground state molecular fragments in gas discharges. These include microwave absorption, infrared absorption, optical emission and laser-induced fluorescence [12]. The measurement of these temperatures can give access to information about the electron impact excitation or dissociative excitation processes as a function of the various interrelated plasma parameters and/or their evolution as a function of the discharge space. Concerning the rotational temperature, the most commonly used experimental technique is the analysis of the intensity distribution in the rotational fine structure of electronic transitions. Among the methods employed for the determination of the rotational temperature from these spectra, use of the Boltzmann plot is the most popular. However, this method may be unreliable in cases in which the rotational structure is not completely resolved. This situation occurs in the case of the emission spectrum of SiH where Λ doubling in the $X^2\Pi$ state, in combination with partial overlapping of the branches, forms an intricate structure which is difficult to resolve entirely. A second method of rotational temperature determination is the simulation of the experimental rotational spectrum. This method requires extensive calculations, but offers the advantage of the incorporation of lines with specific spectral features, such as for example unresolved Λ doubling. Thus, a method of improved accuracy for the determination of T_{ROT} has been developed by this group, with which temperatures in the range 2100–2800 K are obtained, depending on the discharge conditions [13]. More specifically, extended least squares fitting analysis in combination with sufficient spectral resolution, an improved term-value formula and the experimentally determined instrument function of the optical system are used for the determination of a more accurate value of T_{ROT} .

In this study, the rotational temperature of the 0–0 band of the $A^2\Delta-X^2\Pi$ transition of SiH is determined, using the method described above. In fact, the evolution of the rotational temperature in the discharge space and its variation with pressure, both presented for the first time in this work, are examined and compared with the spatial profiles and the variation of the spatially integrated emission intensity.

2. Experimental details

The experimental set-up is described in detail elsewhere [14]. Briefly, the cell is a 160 mm wide stainless steel parallel plate discharge chamber, cylindrical in shape with 55 mm diameter electrodes. The electrode separation was 25 mm in this series of experiments. The pressure is measured by a capacitance manometer and can be adjusted independently of the flow rate, within the region of interest, by using mass-flow controllers and downstream pressure control by a throttling valve. Matheson ultra-high-purity silane was used in all cases. The system was baked out and pumped down to 10^{-7} Torr prior to the experiments.

The chamber is completely characterized from the electrical point of view. The method used for the measurement of the power consumed in the discharge is

described in detail elsewhere [15]. Briefly, the current and voltage waveforms measured outside the reactor are transformed to the equivalent ones at the powered electrode, by using an electrical circuit model with experimentally determined components. The equivalent circuit contains elements that account also for resistive losses.

The method used for the determination of the rotational temperature of SiH* is discussed in [13]. The set-up used for recording spatially resolved emission spectra is schematically shown in figure 1. Namely, two 0.5 mm slits are placed such that there is a distance of 10 cm between them and a lens of 5.5 cm focal length is used to focus the emission collected from a pure silane discharge onto the entrance slit of a 1 m JY-THR1000 monochromator. This configuration provides a spatial integrity of about 0.5 mm at the axis of the chamber, ensuring that the light from a 0.5 mm slice of the plasma is actually gathered. The monochromator is equipped with a 3600 grooves mm^{-1} ruled grating and a side-on PMT. Spatial profiles are obtained by moving the chamber's axis perpendicularly to the static slit–lens system. Finally, the spectrum and the intensity of the 0–0 bandhead (4143.5 Å) are recorded, at specific points of the interelectrode space.

The applicability of the experimental procedure concerning the recording of the spectrum for the determination of the rotational temperature is limited by the total intensity measured at each point. More specifically, there is a bottom limit for the detection system, below which the experimental peak heights are too small and thus unable to provide sufficient data for the calculation of the rotational temperature. In fact, erroneous calculations may come about since in this case a small variation in the recorded peak's height, for instance due to electrical noise superimposed on the signal, turns out to be significant compared with the maximum peak height. Therefore, under the specific experimental conditions of 75 mTorr and 100 V peak-to-peak voltage, the measurements of T_{ROT} start at a distance of 5 mm from the rf electrode and extend out to a distance of 17 mm. The measurements of T_{ROT} as a function of the pressure are performed at the emission's maximum intensity position, which varies with pressure [16]. All the measurements reported here are made under particle-free conditions, verified by a laser-light-scattering technique [13].

3. Results and discussion

The $A^2\Delta$ excited state of the SiH* radical is produced by dissociative excitation of silane through high Rydberg states, via direct one-electron impact [17, 18]. The direct excitation of ground state radicals has been proven experimentally to be negligible [19]. This has also been confirmed by our experimental observations taking into account also that the percentage of ground state SiH radicals among the primary dissociation products is very low [20] and at the same time that the total dissociation of silane has been measured to be 0.5–2% under our conditions [21].

In pure silane radio frequency discharges, the electron energy distribution function includes basically low-energy electrons and a high-energy tail, originating from stochastic

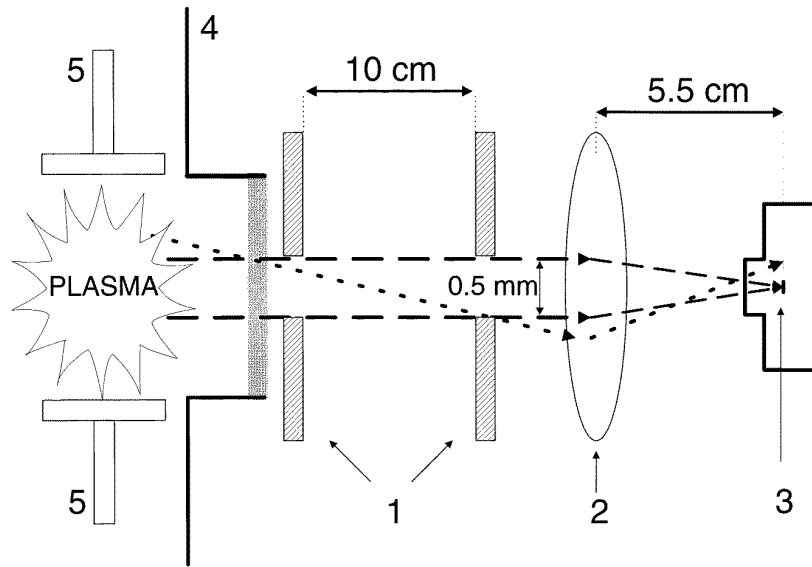
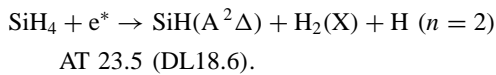
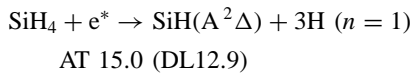
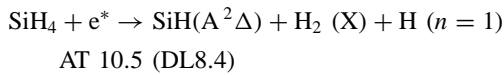


Figure 1. The experimental set-up for spatially resolved optical emission measurements: 1, 0.5 mm slits; 2, 55 mm focal length lens; 3, monochromator entrance slit; 4, plasma chamber; and 5, electrodes.

collisions of electrons with the oscillating plasma sheath's boundary. The dissociative excitation process occurs by impact with electrons having much higher energy than required. Thus, the appearance threshold (AT) and the calculated dissociation limit (DL) for specific dissociation processes have been found as follows [22]:



This excess of energy is imparted to the various dissociation fragments. Thus, a translational energy of the order of several electron-volts has been reported for H atoms, while rotational and vibrational temperatures in the ranges 2000–2800 and 4000–6000 K respectively can be found in the literature [8,9]. In addition, the rotational temperature of the less short-lived, ground state $\text{SiH}(X^2\Pi)$ radical, produced through the analogous electron-impact dissociation of silane, has been reported to be 950 K [23]. These observations distinguish entirely electron-impact dissociative processes from direct excitation from the ground state, for which the rotational temperatures of excited species in various cases have been found to be close to room temperature [24]. In the previous works, however, the dependence of T_{ROT} on the electron impact energy has led to contradictory results. More specifically, utilizing the ability of their multipole dc reactor to generate plasma with monoenergetic electrons, Perrin and Schmitt [25] observed that the intensity distribution of SiH^* appeared to be independent of the primary electron energy and was in no way affected by pressure changes in the mTorr range. On the other hand, Tsurubuchi *et al* [9] observed

a lowering of the rotational temperature from 1700 to 1400 K during electron beam experiments on changing the electron energy from 20 to 500 eV. At the same time, they calculated vibrational temperatures of 3800 and 7800 K for the two cases respectively. This behaviour was attributed to different excitation mechanisms operating at 20 and 500 eV. In another case of an Ar– SiH_4 plasma jet, a rotational temperature of 4000 K and a vibrational temperature of 5600 K were measured [26]. All the above references comprise a controversial picture of the rotational temperature's determination and the factors that influence this measurement. In all these works, however, a low-resolution spectrum was used and thus the values obtained are expected to be inaccurate since deviations in calculations of Λ doubling observed by this group may induce a significant error, as explained in [13].

Measurements of the rotational temperature can be performed on the basis of minimization of the differences between the experimental emission spectrum and a corresponding simulation spectrum. For this, various criteria have been used in the past, such as the minimal surface criterion (MSC) and the homothetic parallelism criterion (HPC) [24].

A least squares fitting (LSF) method is used in this work, for the minimization of the following error function [9]:

$$\varepsilon = \sum_{i=1}^N \left(\frac{I_{i,exp}}{I_{exp}^{max}} - \frac{I_{i,sim}}{I_{sim}^{max}} \right)^2.$$

This method has been used by this group to obtain an improved simulation of the $A^2\Delta-X^2\Pi$ spectrum, by utilizing an improved term-value formula for the calculation of the rotational levels and by optimizing the most recent set of molecular constants [13].

Figure 2 presents the calculated Q_1 branch profile for various T_{ROT} in the range 2200–2600 K. From figure 2, it is obvious that the relative changes of the peak heights, for

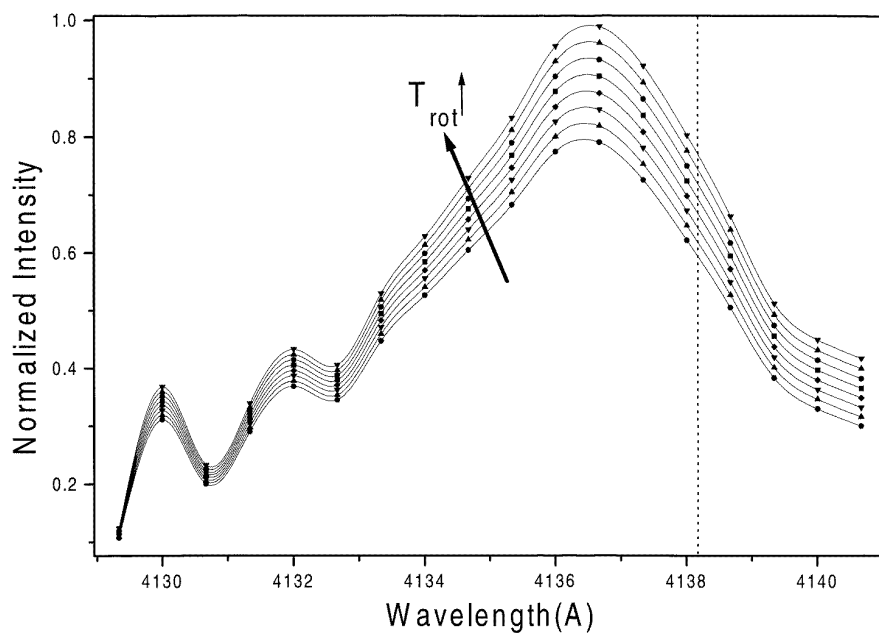


Figure 2. The evolution of the Q_1 branch profile with increasing T_{ROT} from 2200 to 2550 K with an interval of 50 K, calculated from the simulation method.

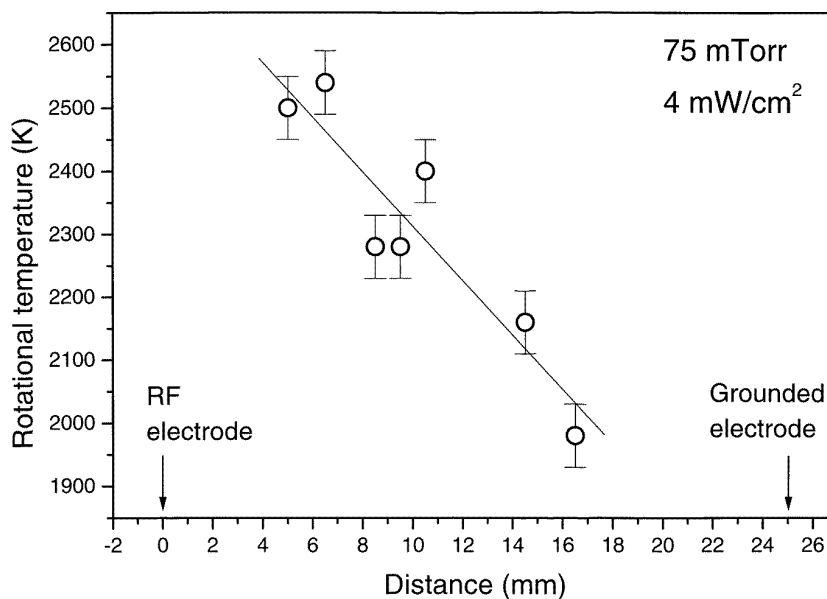


Figure 3. T_{ROT} as a function of the distance from the rf electrode for a 75 mTorr pure silane discharge.

large values of the angular momentum J , namely the tail of the branch beyond 4138 \AA , are more influenced by the increase of the rotational temperature than are those at the beginning of the branch. Two important factors contribute to this behaviour. The first one is the modification of the population distribution in the rotational levels due to the respective change of the rotational temperature; the second is the influence of Λ doubling on the observed peak heights as a result of the convolution of adjacent Λ doublets. Namely, it is known [27] that the Λ -doubling components of the $^2\Pi_{1/2}$ multiplet are separate at low J , form a single

blended line at $J = 10.5$ and $J = 11.5$ while crossing one another and re-emerge into separated lines for larger J . This means that the more accurate the calculations for large quantum numbers, J , the more sensitive and accurate the measurement. However, the calculated term values, the prediction of Λ doubling and possible pre-dissociation phenomena result in a less efficient simulation of the spectrum in the region $J > 13$, beyond 4138 \AA . Thus, the measurements of the rotational temperature presented here are based on the first 12 peaks of the Q_1 branch. This is for two reasons. First, the simulation of the emission

spectrum in the specific region by means of Λ doubling and the calculation of rotational levels is very good, as the small values of the error function indicate. Second, in order to include the R_1 branch in the calculation as proposed in [5], the recording of the experimental spectrum in a wavelength region three times larger is required. Furthermore, a comparison of rotational temperature measurements in these two cases has led to exactly the same results. Thus, R_1 branch peaks are excluded from the calculation.

Figure 3 presents the variation of the rotational temperature in the interelectrode space, for 75 mTorr pure silane discharges, determined by the simulation method described above. T_{ROT} appears to decrease linearly as the distance from the rf sheath region increases. Namely, a maximum value of around 2500 ± 50 K is measured at 5 mm whereas a minimum value of 1980 ± 50 K is obtained at 17 mm. Since the main electron-heating mechanism under these conditions is related to the periodic expansion of the sheath boundary, the electrons possessing more energy than 10.5 eV and thus capable of producing $\text{SiH}(A^2\Delta)$ are created near the sheath region. Therefore, the effective electron density, namely the density of electrons having energy higher than the appearance threshold of the species, is reduced with the distance from the rf electrode sheath, because Joule heating in the bulk is considered to play a minor role. Indeed, it has been found that the electron energy for molecular gases at low pressures falls rapidly away from the electrode [28]. This indicates that the rotational temperature is sensitive to the variation of the excess energy of the electrons. More specifically, it is generally accepted that less than 10% of the total excess energy goes for the rovibrational excitation of SiH [11]. This excess energy measured as T_{ROT} reflects directly the energy content of the electrons having more energy than 10.5 eV. Bearing this in mind, the results presented here are interpreted considering that there is a simple analogy between T_{ROT} and the mean electron energy, provided that the shape of the EEDF does not change. This rationale is also confirmed by the pressure-dependence behaviour of T_{ROT} presented later.

It can be observed in figure 4, in which a Boltzmann EEDF is plotted for three arbitrary values of the mean electron energy together with the SiH^* cross section [9], that the effective electron density (plotted in the inset) decreases exponentially with decreasing mean electron energy. Following the reasoning mentioned above, the observed linear decrease of T_{ROT} indicates that the change of mean electron temperature exhibits a similar linear decrease. However, the calculated effective electron energy dependence over a wider range than that plotted in the inset of figure 4 exhibits a strongly exponential behaviour. In order to obtain a linear dependence, like the one observed here, one must consider that the change of $k_\beta T_e$ is in a range smaller than the one plotted here. In other words, the value of $k_\beta T_e$ assuming a Maxwell-Boltzmann distribution is expected to change by less than 0.5 eV in the interelectrode space. In this way, the spatial variation of T_{ROT} can provide qualitative information on the relative change of the mean electron energy in the interelectrode space, provided that the shape of the EEDF does not change significantly.

The results presented here are compatible with electrical probe measurements in silane radio frequency discharges, where values of $k_\beta T_e = 2\text{--}2.5$ eV were obtained [29]. More recently, Lin *et al* [30] used a tuned and heated Langmuir probe to obtain mean electron energies in the range 1.5–5 eV on varying the power from 20 to 40 W at a constant pressure of 150 mTorr. These observations provide additional confirmation of the validity of the method.

However, the lack of data on the precise dependence of the rovibrational excitation on the electron impact energy makes the quantitative interpretation of such experimental results difficult. Furthermore, the data provided by Lin *et al* cannot be used as a reference because the power consumption in their work is probably measured by a SWR bridge.

Besides the decrease of the excess energy, measured as T_{ROT} and attributed to a similar decrease of the mean electron energy, the number density of the species will also be affected. Indeed, as one can observe in figure 5, which presents the spatial emission intensity distribution of SiH^* under the same experimental conditions, the spatial profile exhibits a maximum 7 mm away from the powered electrode and a relatively narrow intensity distribution. The dark region of the glow corresponding to almost zero intensity extends 3 mm away from the powered electrode and 5 mm from the grounded electrode. The reason for the non-zero intensity in the dark region is that the sheath's boundary is curved around the electrode and this region of high-energy electrons is in the line of sight of the dark space. It is observed that the light intensity is not symmetrical relative to the midgap; this is due to our discharge's geometry. In addition, the absence of the grounded electrode's sheath is consistent with the monotonic decline of the rotational temperature profile, since a supplementary sheath electron-heating mechanism in the grounded electrode's area is expected to modify the observed profile.

An interesting observation can be made by comparing figures 3 and 5. The highest rotational temperature has been recorded for a distance of 5 mm from the rf electrode, whereas the maximum emission intensity is further away, at 7 mm distance. This is an indication that the 5 mm region is richer in high-energy electrons; however, the effective electron density is lower than the one at 7 mm. Several factors can contribute to this phenomenon, such as for example the antagonistic dissociative ionization of silane and mainly the fact that the total electron density, which also affects the effective electron concentration, at 5 mm is much lower than that at 7 mm distance. In fact, an increase of the electron density, at the same mean electron energy, would induce a linear increase of the effective electron density. This is in good agreement with the observed increase of the emission intensity on going from 3 mm to the 7 mm maximum in figure 5. Thus, following the reasoning mentioned above, one expects a small decrease of the mean electron energy on going from 5 to 7 mm accompanied by a drastic increase of the electron density. In fact, the observed emission intensity profile must be considered the result of the combination of the lowering of the mean electron energy on moving away from

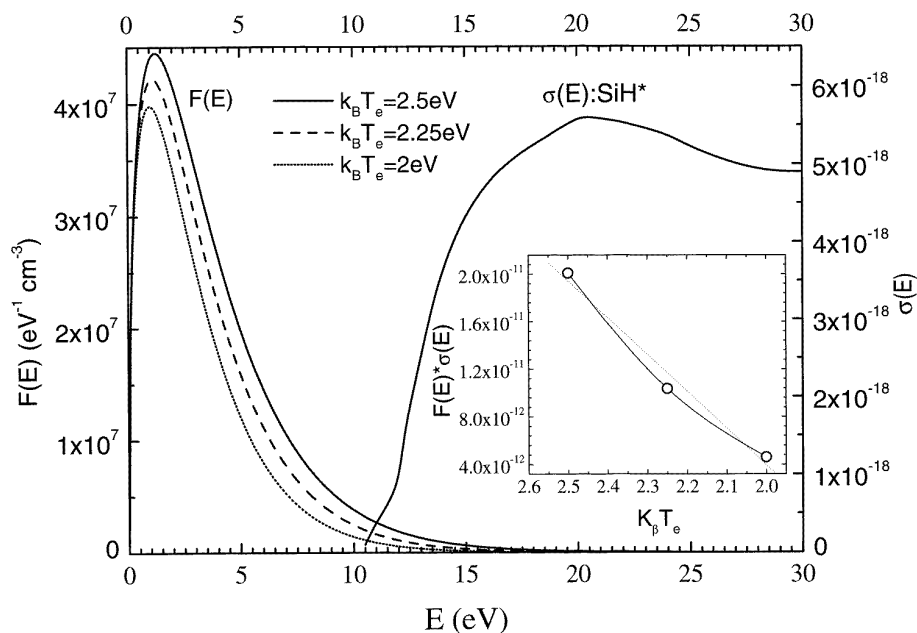


Figure 4. Calculated Maxwell–Boltzmann distributions for three arbitrary values of the mean energy and $\text{SiH}(A^2\Delta)$ cross section as functions of the electron energy. The variation of the convolution $F(E)\sigma(E)$ is shown in the inset.

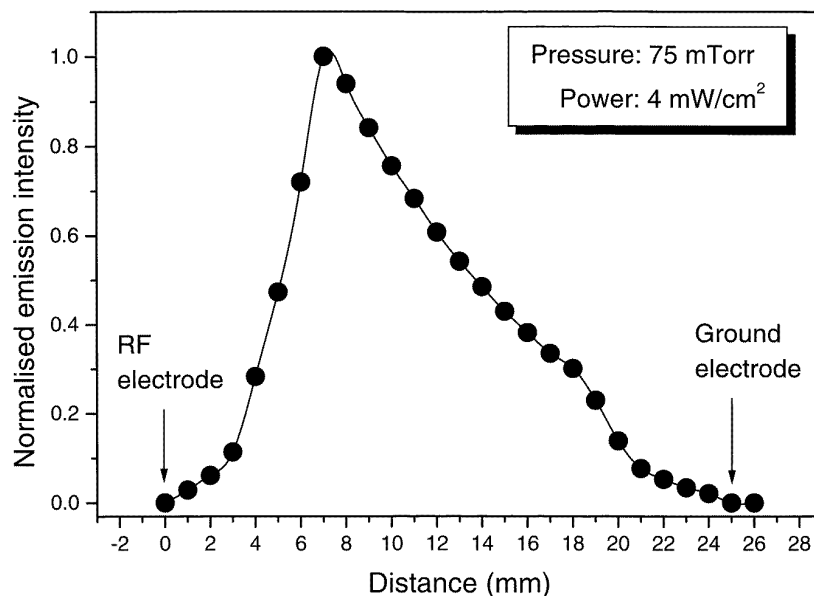


Figure 5. The spatially resolved SiH^* emission intensity as a function of the distance from the rf electrode for a 75 mTorr pure silane discharge.

the sheath region and the spatial variation of the electron density. Bearing this in mind, one may also conclude that the change in the electron density is less steep beyond 7 mm to account for the emission profile being less steep, given the monotonic decline of the rotational temperature profile.

The variation of the rotational temperature with pressure under constant peak-to-peak voltage (100 V) was also examined (figure 6). The measurements are performed at the point of maximum intensity in the interelectrode space, determined from emission spatial intensity distribution measurements, because it changes

with pressure, namely it moves towards the rf electrode. A decrease of rotational temperature is observed with increasing pressure. More specifically, the value of 2440 ± 50 K, obtained at 38 mTorr, decreases to 2260 ± 50 K at 200 mTorr. The observed behaviour is due to the expected decrease of the mean electron energy as the number of electron–molecule collisions increases with the pressure. This result is also in very good agreement with the variation of the mean electron energy as a function of pressure presented by Lin *et al* [30]. More specifically, they measured a decrease of the mean electron energy

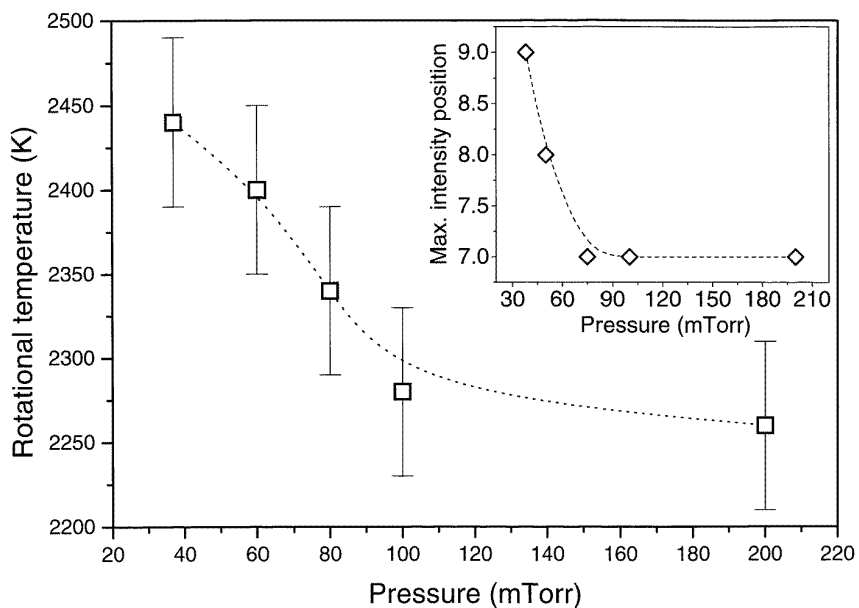


Figure 6. T_{ROT} as a function of the discharge pressure at the maximum-intensity position for constant $V_{pp} = 100$ V. The position of the maximum intensity in the interelectrode space as a function of the pressure is shown in the inset.

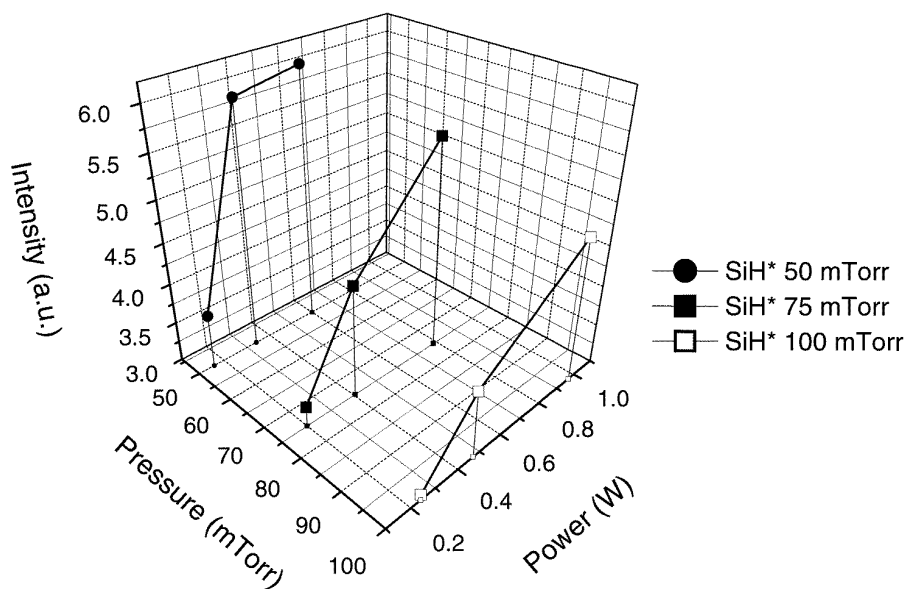


Figure 7. Overall emission intensities of SiH* as a function of the pressure and power.

from 5.23 to 4.92 eV on varying the pressure from 150 to 300 mTorr. This 0.3 eV difference is in agreement with the rationale supported earlier, concerning the sensitivity of the method. In addition, the trend of the mean electron energy with pressure exhibits a similar behaviour to that of the rotational temperature, tending to saturate at higher pressures. However, the interpretation is still qualitative and an absolute comparison of differences in rotational temperature values and mean electron energies is difficult.

The integral of the emission intensity over the interelectrode space is plotted in figure 7, for three excitation voltages, namely 80, 100 and 120 V, as a

function of the pressure and the power actually consumed in the discharge. One can observe that the decrease of the overall emission intensity with the pressure is more pronounced at higher peak-to-peak voltages, indicating that the changes in the mean electron energy and/or electron density occur mostly in the area of the rf sheath. This is in agreement with earlier observations by this group concerning power dissipation in pure silane discharges [31,32]. More specifically, in the case of increasing pressure the observed increase of the dissipated power is due to the combination of a greater electron density and a greater number of collisions. This leads to a decrease

of the capacitive reactance as a result of the decrease in sheath length (inset to figure 6). In contrast to the case of increasing pressure, for which the electron temperature is expected to drop [30], the increase of power dissipation due to the increase of V_{pp} represents basically the increase of the net current flow, whereas the electron temperature is expected to be slightly effected.

To sum up, measurement of the rotational temperature determined from the emission spectrum of the $A^2\Delta \rightarrow X^2\Pi$ transition of SiH appears to be a sensitive probe of the mean electron energy. The use of a method of improved accuracy for rotational temperature measurements is a critical parameter in this approach.

4. Conclusions

The variation of the rotational temperature in the interelectrode space and with the pressure is reported for the first time. A linear decrease of the rotational temperature is observed on moving from the powered to the grounded electrode. The results are compared with spatial emission intensity profiles and a difference between the positions of maximum emission intensity and maximum T_{ROT} is observed. The dependence of T_{ROT} on the pressure is investigated at the point of maximum emission intensity and a decrease of T_{ROT} with increasing pressure is observed.

A detailed examination of these observations has revealed that the rotational temperature value is a sensitive measure of the excess energy imparted to the fragment as rovibrational excitation during the one-electron-impact dissociative excitation of silane. Thus, a simple analogy between T_{ROT} and the mean electron energy is adopted, considering that the shape of the EEDF does not change significantly. These observations are compatible with electrical probe measurements.

Concerning the spatially resolved (axial direction) emission intensity profiles, it is demonstrated that, in conjunction with rotational temperature measurements, information about the distribution of the electron density in space can be deduced. The idea is that T_{ROT} presents a maximum where the mean electron energy is maximum, whereas the emission presents a maximum at the point of maximum effective electron density which is generally [31] a function both of the total electron density and of the mean electron energy.

Furthermore, space-integrated emission intensities under various discharge conditions are presented. More specifically, it is shown that the overall emission intensity increases with the power under constant pressure, reflecting mainly the increase of the net current flow, and decreases with the pressure under a constant peak-to-peak voltage, as a result of the modification of the discharge's impedance.

To sum up, the method presented in this work comprises a valuable non-perturbing means of investigating the electron kinetics in silane-containing discharges. In fact, this is the only method, as far as we know, that can extract information about the variations of the mean

electron energy and the electron density in the interelectrode space. However, a quantitative approach is difficult at this point since there is a lack of data concerning the exact dependence of T_{ROT} on the excess energy.

References

- [1] Bruno G, Capezzuto P and Madan A 1995 *Plasma Deposition of Amorphous Silicon Based Materials* (San Diego: Academic)
- [2] d'Agostino R, Favia P and Fracassi F 1997 *Plasma Processing of Polymers, (NATO ASI Series)* (Dordrecht: Kluwer)
- [3] Hamma S and Roca i Cabarrocas P 1997 *Thin Solid Films* **296** 11
- [4] Djurovic S, Roberts J R, Sobolewski M A and Olthoff J K 1993 *J. Res. NBS* **98** 159
- [5] Tochikubo F, Suzuki A, Kakuta S, Terazono Y and Makabe T 1990 *J. Appl. Phys.* **68** 5532
- [6] Petrovic Z L, Tochikubo F, Kakuta S and Makabe T 1993 *J. Appl. Phys.* **73** 2163
- [7] Radovanov S B, Tomcik B, Petrovic Z L and Jelenkovic B M 1990 *J. Appl. Phys.* **67** 97
- [8] Perrin J and Delafosse E 1980 *J. Phys. D: Appl. Phys.* **13** 759
- [9] Tsurubuchi S, Motohashi K, Matsuoka S and Arikawa T 1992 *Chem. Phys.* **61** 493
- [10] Perrin J and Schmitt J P M 1984 *Chem. Phys. Lett.* **112** 69
- [11] Perrin J 1993 *J. Phys. D: Appl. Phys.* **26** 1662
- [12] Knights J C, Schmitt J P M, Perrin J and Guelachvili G 1982 *J. Chem. Phys.* **76** 3414
- [13] Stamou S, Mataras D and Rapakoulias D 1997 *Chem. Phys.* **218** 57
- [14] Mataras D, Cavadias S and Rapakoulias D 1993 *J. Vac. Sci. Technol. A* **11** 664
- [15] Spiliopoulos N, Mataras D and Rapakoulias D E 1996 *J. Vac. Sci. Technol. A* **14** 2757
- [16] Mataras D, Cavadias S and Rapakoulias D 1989 *J. Appl. Phys.* **66** 119
- [17] Winstead C, Pritchard H P and McKoy V 1994 *J. Chem. Phys.* **101** 338
- [18] Pinnaduwaige L A and Datskos P G 1997 *J. Appl. Phys.* **81** 7715
- [19] Kampas F J and Griggith R W 1981 *J. Appl. Phys.* **52** 1285
- [20] Doyle J R, Doughty D A and Gallagher A 1990 *J. Appl. Phys.* **68** 4375
- [21] Spiliopoulos N, Mataras D and Rapakoulias D 1997 *J. Electrochem. Soc.* **144** 634
- [22] Perrin J and Aarts J F M 1983 *Chem. Phys.* **80** 351
- [23] Schmitt J P M, Gressier P, Krishnan M, de Rosny G and Perrin J 1984 *Chem. Phys.* **84** 281
- [24] Chelouah A, Marode E, Hartmann G and Achat S 1994 *J. Phys. D: Appl. Phys.* **27** 940
- [25] Perrin J and Schmitt J P M 1981 *Chem. Phys.* **67** 167
- [26] Meeusen G J, Ershov-Pavlov E A, Meulenbroeks R F G, van de Sanden M C M and Schram D C 1992 *J. Appl. Phys.* **71** 4156
- [27] Brown J M and Robinson D 1984 *Mol. Phys.* **51** 883
- [28] Kushner M J 1983 *J. Appl. Phys.* **54** 4958
- [29] Mosburg E R Jr, Kerns R C and Abelson J R 1983 *J. Appl. Phys.* **54** 4916
- [30] Lin Q, Lin X, Yu Y, Wang H and Chen J 1993 *J. Appl. Phys.* **74** 4899
- [31] Spiliopoulos N, Mataras D and Rapakoulias D 1997 *Appl. Phys. Lett.* **71** 605
- [32] Mataras D, Coutelieris F, Kounavis P and Rapakoulias D E 1996 *J. Phys. D: Appl. Phys.* **29** 2452